

Influence of the substitution pattern on exciton localisation in centrosymmetric quadrupolar dyes

Chinju Govind^a, Kamil Skonieczny^b, Daniel T. Gryko^{*b}, and Eric Vauthey^{*a}

^aDepartment of Physical Chemistry, University of Geneva, 30 Quai Ernest-Ansermet, CH-1211 Geneva 4, Switzerland. E-mail: eric.vauthey@unige.ch

^bInstitute of Organic Chemistry, Polish Academy of Sciences, Kasprzaka 44/52, 01-224 Warsaw, Poland. E-mail: daniel.gryko@icho.edu.pl

Contents

S1 Additional Experimental Details	4
S1.1 Synthesis of A1 and characterisation	4
S2 Weller equation	5
S3 Additional results	5
S3.1 Stationary electronic spectroscopy	5
S3.2 Time-resolved fluorescence	7
S3.3 Stationary vibrational spectroscopy	7
S3.4 Quantum-chemical calculations	8
S3.5 Electronic transient absorption spectroscopy	9
S3.6 Time-resolved IR spectroscopy	11

List of Figures

S1	Synthesis of A1	4
S2	¹ H-NMR spectrum of A1 Synthesis of A1	5
S3	¹³ C-NMR spectrum of A1 Synthesis of A1	5
S4	Absorption (A, C) and emission (B, D) solvatochromism of A1 (A, B) and C1 (C,D). For the absorption (A,C), the transition energy is plotted vs. the solvent polarisability function, $f(n^2)$, to highlight dispersion interactions. For emission (B, D), the transition energy is plotted vs. the orientational polarisation function of the solvent to evidence dipole-dipole interactions. CHX: cyclohexane; TOL: toluene; DEE: diethyl ether; DBE: dibutyl ether; THF: tetrahydrofuran; BCN: benzonitrile.	6
S5	Stationary electronic absorption and emission spectra of (A) A2 and (B) C2 in cyclohexane (CHX) and benzonitrile (BCN) and of (C) the single-branched C2sb in cyclohexane and dimethylsulfoxide (DMSO).	6
S6	Stationary IR absorption spectra of (A) A1 and (B) C1 in toluene.	7
S7	Energy of the ground state and Franck-Condon excited state of (A) A1 and (B) C1 as a function of the dihedral angle between the DPND core and the phenyl ring of one of the donors, calculated at the CAM-B3LYP/6-31g(d,p) level. The gray dashed lines represent the thermal energy, $k_B T$, at room temperature.	8
S8	Frontier molecular orbitals (CAM-B3LYP/6-31G(d,p)) of analogues of A2 and C2 with R=H involved in the $S_1 \leftarrow S_0$ (HOMO to LUMO) and $S_2 \leftarrow S_0$ (HOMO-1 to LUMO) transitions.	8
S9	Transient absorption spectra measured at various time delays after 600 nm excitation of A1 and 640 nm excitation of C1 in cyclohexane and benzonitrile.	9
S10	Top: Transient absorption spectra measured at various time delays after 565 nm excitation of A2 in cyclohexane and benzonitrile. Bottom: Evolution-associated difference absorption spectra and time constants obtained from global analysis assuming a series of successive exponential steps (A→B→C→). The negative stationary absorption and stimulated emission spectra are shown in shaded area for comparison.	10
S11	Top: Transient absorption spectra measured at various time delays after 600 nm excitation of C2 in cyclohexane and benzonitrile. Bottom: Evolution-associated difference absorption spectra and time constants obtained from global analysis assuming a series of successive exponential steps (A→B→C→). The negative stationary absorption and stimulated emission spectra are shown in shaded area for comparison.	10
S12	Time-resolved IR absorption spectra measured at various time delays after 600 nm excitation of A1 in cyclohexane, toluene, tetrahydrofuran, benzonitrile and a 80:20 (v/v) dimethylsulfoxide/benzonitrile mixture.	11
S13	Time-resolved IR absorption spectra measured at various time delays after 640 nm excitation of C1 in cyclohexane, toluene, tetrahydrofuran, benzonitrile and dimethylsulfoxide.	12
S14	Left: time-resolved IR absorption spectra measured at various time delays after 565 nm excitation of A2 in cyclohexane and dimethylsulfoxide. Right: Evolution-associated difference absorption spectra and time constants obtained from global analysis assuming a series of successive exponential steps (A→B→C→).	13
S15	Left: time-resolved IR absorption spectra measured at various time delays after 600 nm excitation of C2 in cyclohexane and dimethylsulfoxide. Right: Evolution-associated difference absorption spectra and time constants obtained from global analysis assuming a series of successive exponential steps (A→B→C→).	13

List of Tables

- S1 Fluorescence lifetimes, τ_{fl} , of the dyes in various solvents, and fluorescence quantum yields, Φ_{fl} , in DCM (from ref. 1,2). Error on τ_{fl} : $\pm 5\%$ 7
- S2 Energy, E , and oscillator strength, f , of the first two electronic transitions of analogues of **An** and **Cn** with R=H obtained from time-dependent DFT calculations at the CAM-B3LYP/6-31G(d,p) level. 9

S1 Additional Experimental Details

S1.1 Synthesis of A1 and characterisation

All chemicals were used as received unless otherwise noted. The reagent 4-ethynyl-N,N-dimethylaniline was purchased from Astatech, Inc., copper(I) iodide from Sigma-Aldrich, tetrakis(triphenylphosphine)palladium(0) from BLDpharm, and triethylamine from Chempur.

All reported ^1H NMR and ^{13}C NMR spectra were recorded on 500 or 600 MHz spectrometer. Chemical shifts (δ ppm) were determined with TMS as the internal reference; J values are given in Hz. Mass spectra were obtained via APCI MS. For HRMS measurements both quadruple and TOF mass analyzer types were used. Chromatography was performed on silica (Kieselgel 60, 200–400 mesh).

1,7-Bis((4-(dimethylamino)phenyl)ethynyl)-6,12-diheptyl-5H,11H-dipyrrolo[1,2-b:1',2'-g][2,6]naphthyridine-5,11-dione (A1)

In a Schlenk flask containing a magnetic stirring bar were placed: **1a** (75 mg, 0.11 mmol), CuI (2 mg, 0.01 mmol), Pd(PPh₃)₄ (13 mg, 0.01 mmol), and 4-ethynyl-N,N-dimethylaniline (42 mg, 0.29 mmol). The vessel was evacuated and backfilled with argon (3 times) and anhydrous, degassed toluene was added (15 mL) followed by dry triethylamine (5 mL). The content of the flask was stirred for 48 h at 90 °C. The mixture was transferred to the separatory funnel and the organic layer was washed with degassed water (3 × 25 mL) and brine. The organic layer was then dried over MgSO₄ and the solvent was evaporated with Celite. The target product was purified by silica gel chromatography using toluene/hexanes (2/1) solution as eluent and recrystallized by slow addition of hexane to a solution of the dye in a small amount of dichloromethane. Yield: 35 mg (38%). Dark blue powder; ^1H NMR (500 MHz, CDCl₃) δ 7.85 (d, J = 3.2 Hz, 2H), 7.41 (d, J = 8.7 Hz, 4H), 6.68 (d, J = 8.5 Hz, 4H), 6.64 (d, J = 3.3 Hz, 2H), 3.82 (s, 4H), 3.02 (s, 12H), 1.81 – 1.72 (m, 4H), 1.62 – 1.55 (m, 4H), 1.41 – 1.30 (m, 4H), 1.25 – 1.19 (m, 8H), 0.83 (t, J = 6.4 Hz, 6H); ^{13}C NMR (125 MHz, CDCl₃) δ 158.2, 150.3, 145.6, 132.7, 131.8, 121.9, 120.0, 114.7, 114.3, 111.8, 109.8, 99.6, 83.6, 40.2, 32.0, 30.4, 30.2, 29.9, 29.5, 22.6, 14.2; HRMS (APCI): calcd for C₄₈H₅₅N₄O₂ [M+H]⁺ 719.4325, found 719.4326.

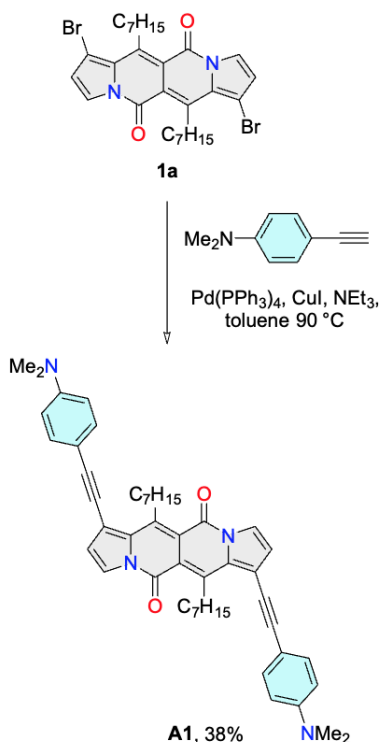


Figure S1 Synthesis of A1.

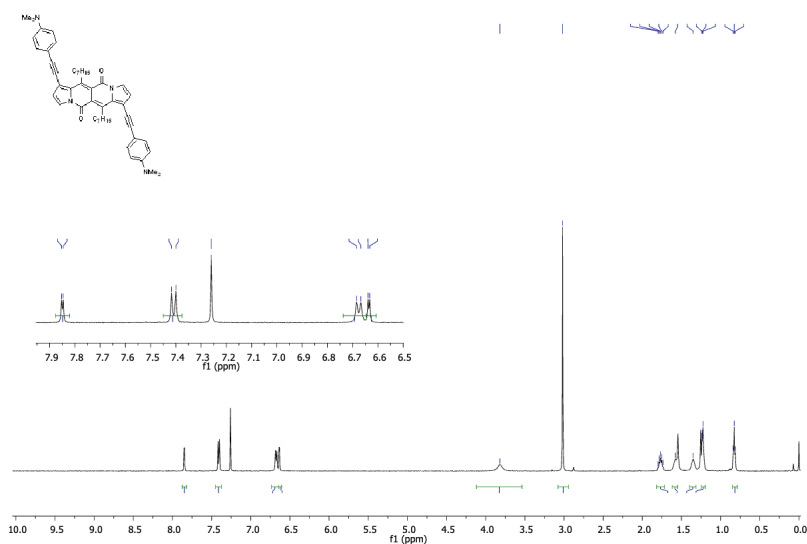


Figure S2 ^1H -NMR spectrum of **A1** Synthesis of **A1**.

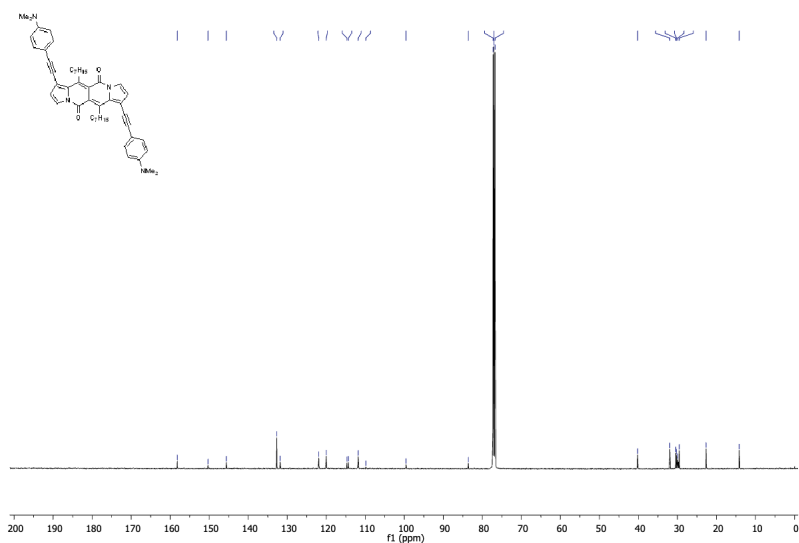


Figure S3 ^{13}C -NMR spectrum of **A1** Synthesis of **A1**.

S2 Weller equation

The driving force of a photoinduced electron transfer process, ΔG_{ET} , can be estimated from the Weller equation:³

$$\Delta G_{\text{ET}} = -E^* + e[E(D^+/D) - E(A/A^-)] + C, \quad (\text{S1})$$

where E^* is the energy of the S_1 state, $E(D^+/D)$ and $E(A/A^-)$ the oxidation and reduction potentials of the electron donor and acceptor, respectively, and C a Coulombic correction factor, which can, in a first approximation, be neglected in highly polar solvents.

S3 Additional results

S3.1 Stationary electronic spectroscopy

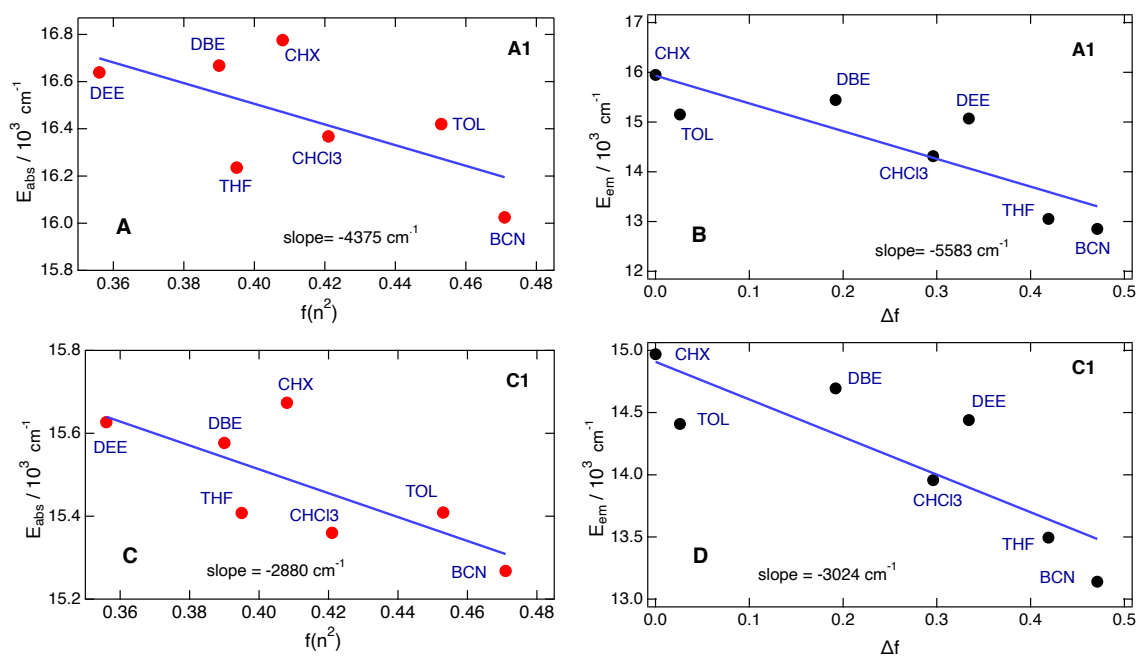


Figure S4 Absorption (A, C) and emission (B, D) solvatochromism of **A1** (A, B) and **C1** (C, D). For the absorption (A, C), the transition energy is plotted vs. the solvent polarisability function, $f(n^2)$, to highlight dispersion interactions. For emission (B, D), the transition energy is plotted vs. the orientational polarisation function of the solvent to evidence dipole-dipole interactions. CHX: cyclohexane; TOL: toluene; DEE: diethyl ether; DBE: dibutyl ether; THF: tetrahydrofuran; BCN: benzonitrile.

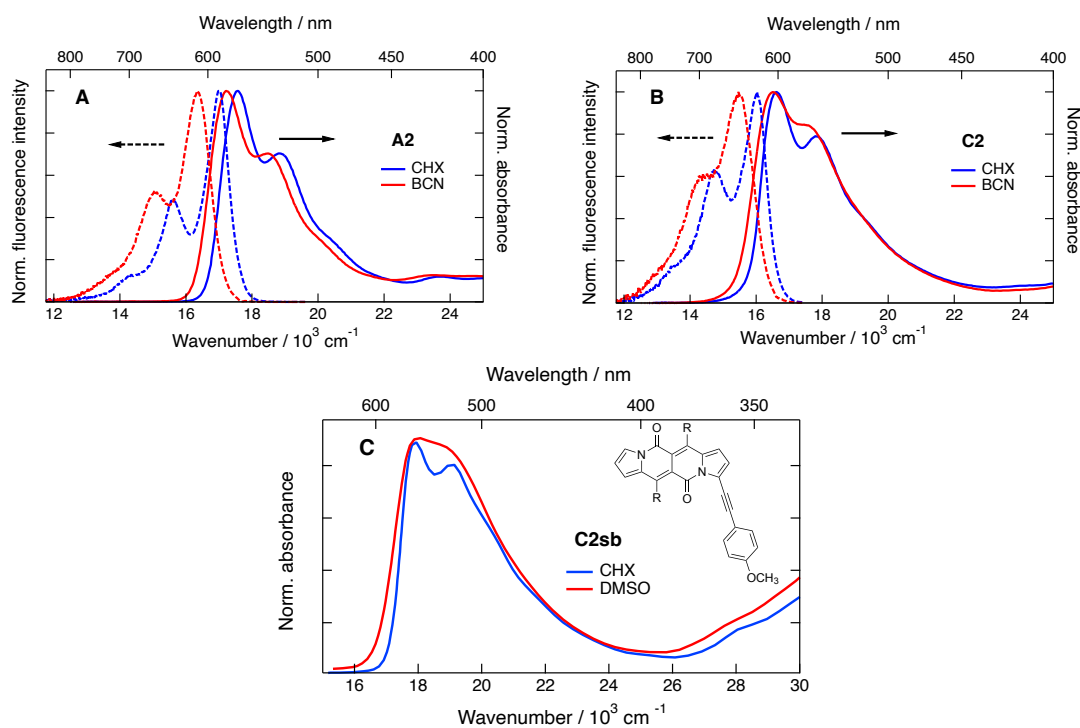


Figure S5 Stationary electronic absorption and emission spectra of (A) **A2** and (B) **C2** in cyclohexane (CHX) and benzonitrile (BCN) and of (C) the single-branched **C2sb** in cyclohexane and dimethylsulfoxide (DMSO).

S3.2 Time-resolved fluorescence

Table S1 Fluorescence lifetimes, τ_{fl} , of the dyes in various solvents, and fluorescence quantum yields, Φ_{fl} , in DCM (from ref. 1,2). Error on τ_{fl} : $\pm 5\%$.

Dye	solvent	τ_{fl} / ns	Φ_{fl} in DCM
A1	CHX	2.6	
	THF	0.49	
C1	CHX	2.8	
	THF	1.5	0.17 ^a
A2	CHX	2.9	
	BCN	2.9	0.59 ^b
C2	CHX	3.1	
	BCN	3.1	0.96 ^b

^{a)} from ref. 1; ^{b)} from ref. 2

S3.3 Stationary vibrational spectroscopy

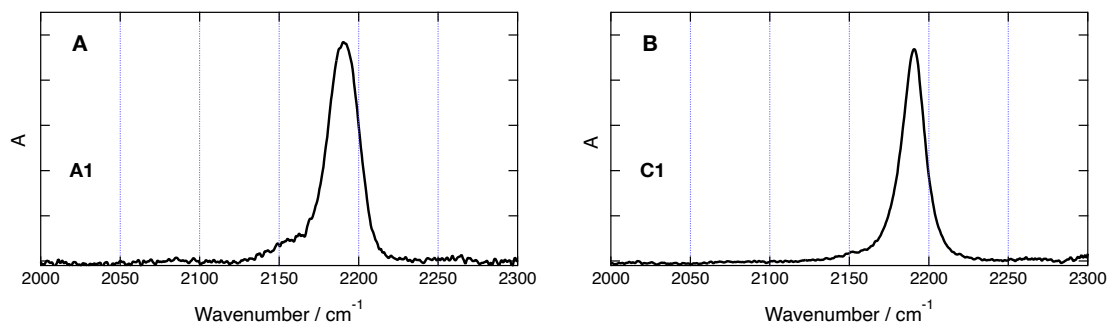


Figure S6 Stationary IR absorption spectra of (A) **A1** and (B) **C1** in toluene. .

S3.4 Quantum-chemical calculations

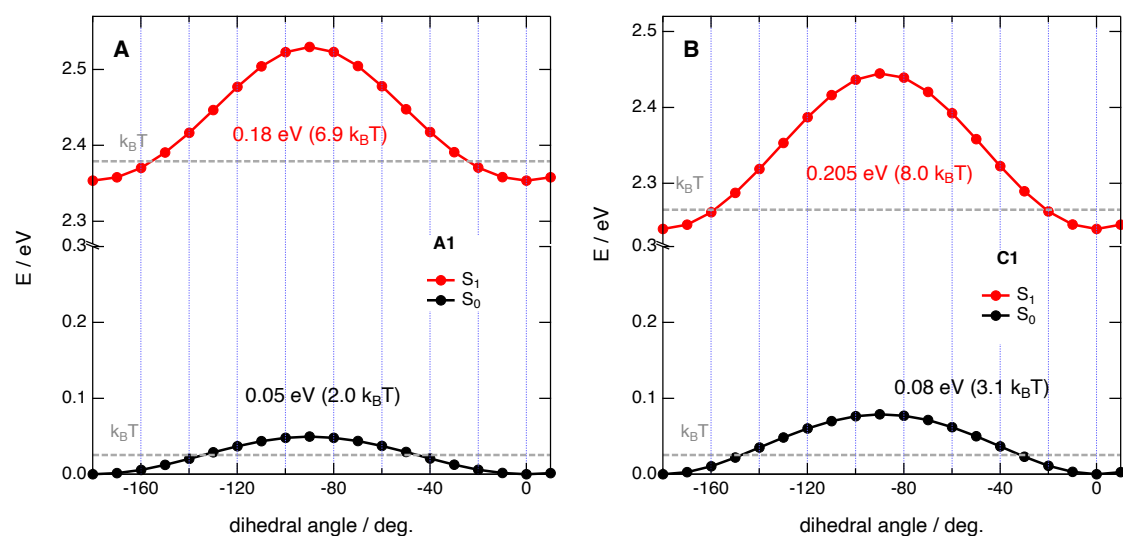


Figure S7 Energy of the ground state and Franck-Condon excited state of (A) **A1** and (B) **C1** as a function of the dihedral angle between the DPND core and the phenyl ring of one of the donors, calculated at the CAM-B3LYP/6-31g(d,p) level. The gray dashed lines represent the thermal energy, $k_B T$, at room temperature.

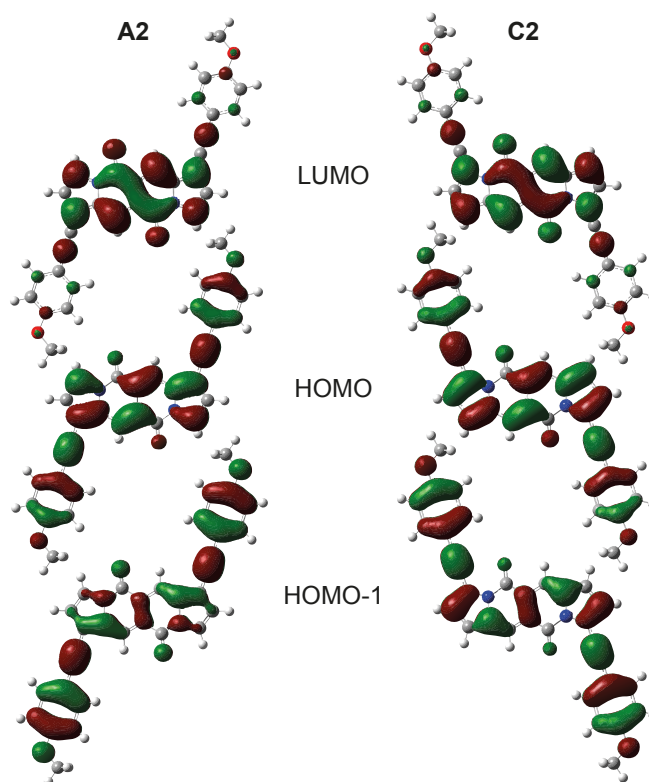


Figure S8 Frontier molecular orbitals (CAM-B3LYP/6-31G(d,p)) of analogues of **A2** and **C2** with R=H involved in the $S_1 \leftarrow S_0$ (HOMO to LUMO) and $S_2 \leftarrow S_0$ (HOMO-1 to LUMO) transitions.

Table S2 Energy, E , and oscillator strength, f , of the first two electronic transitions of analogues of **A_n** and **C_n** with R=H obtained from time-dependent DFT calculations at the CAM-B3LYP/6-31G(d,p) level.

	A1	C1	A2	C2
$S_1 \leftarrow S_0$ (HOMO to LUMO)				
E / eV	2.35	2.24	2.45	2.33
f	1.58	1.49	1.38	1.30
$S_2 \leftarrow S_0$ (HOMO-1 to LUMO)				
E / eV	3.05	2.84	3.24	2.96
f	0	0	0	0

S3.5 Electronic transient absorption spectroscopy

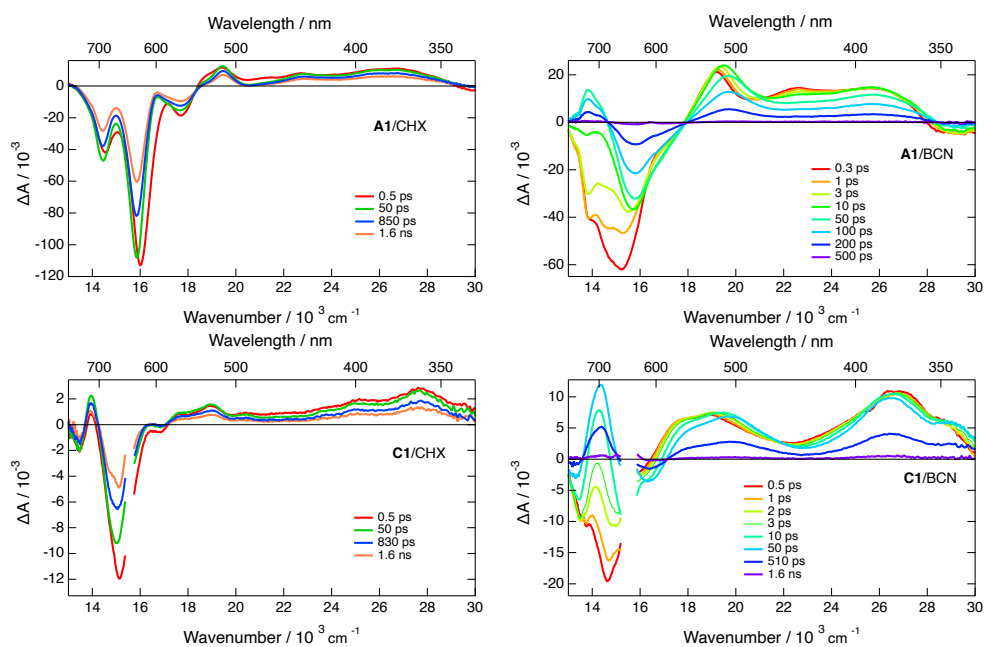


Figure S9 Transient absorption spectra measured at various time delays after 600 nm excitation of **A1** and 640 nm excitation of **C1** in cyclohexane and benzonitrile.

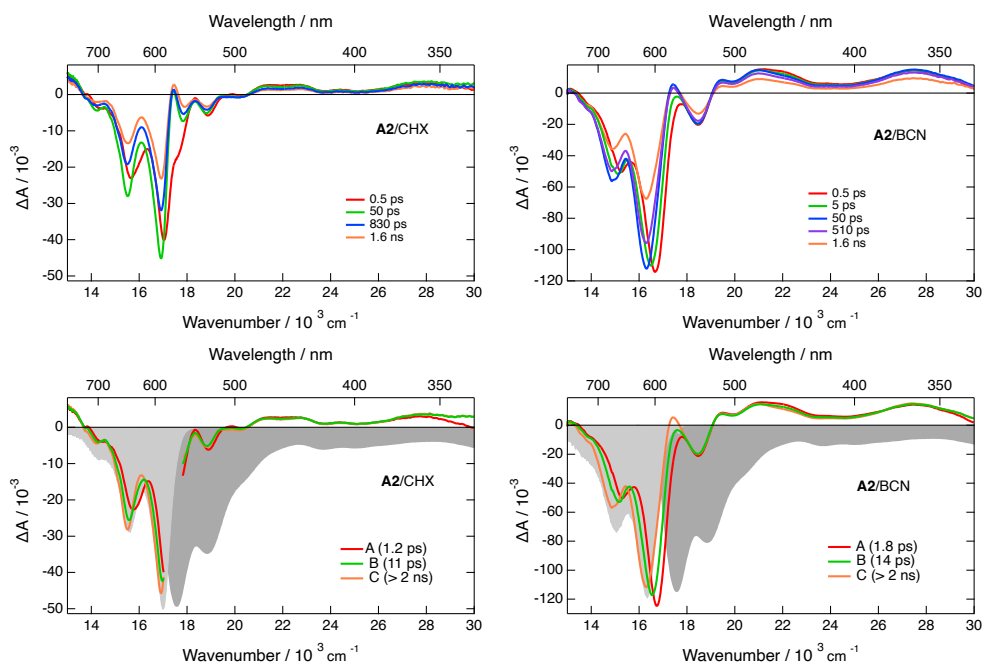


Figure S10 Top: Transient absorption spectra measured at various time delays after 565 nm excitation of **A2** in cyclohexane and benzonitrile. Bottom: Evolution-associated difference absorption spectra and time constants obtained from global analysis assuming a series of successive exponential steps (A→B→C→). The negative stationary absorption and stimulated emission spectra are shown in shaded area for comparison.

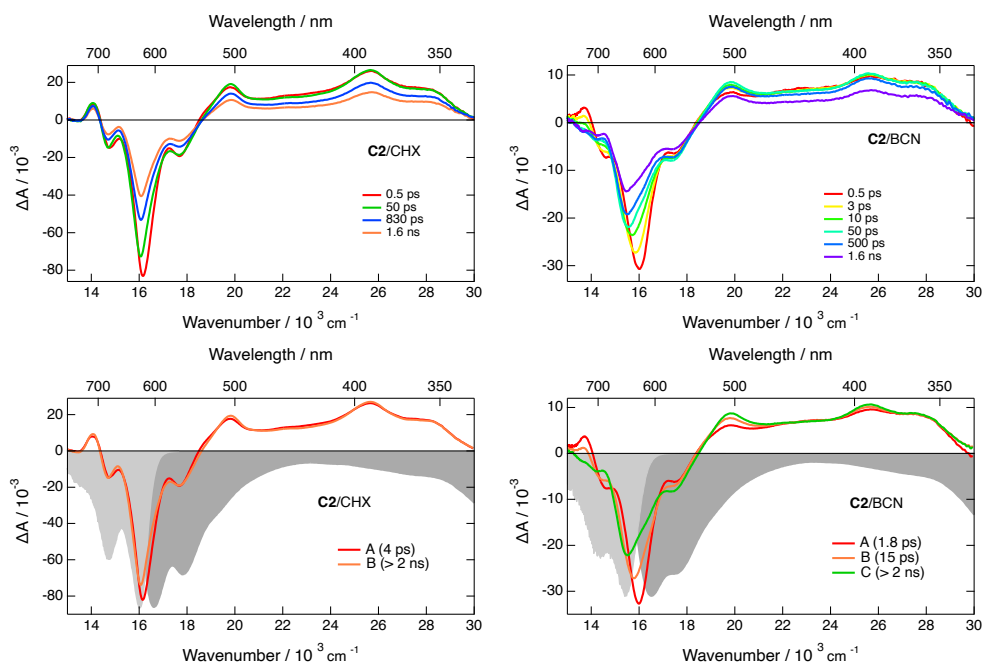


Figure S11 Top: Transient absorption spectra measured at various time delays after 600 nm excitation of **C2** in cyclohexane and benzonitrile. Bottom: Evolution-associated difference absorption spectra and time constants obtained from global analysis assuming a series of successive exponential steps (A→B→C→). The negative stationary absorption and stimulated emission spectra are shown in shaded area for comparison.

S3.6 Time-resolved IR spectroscopy

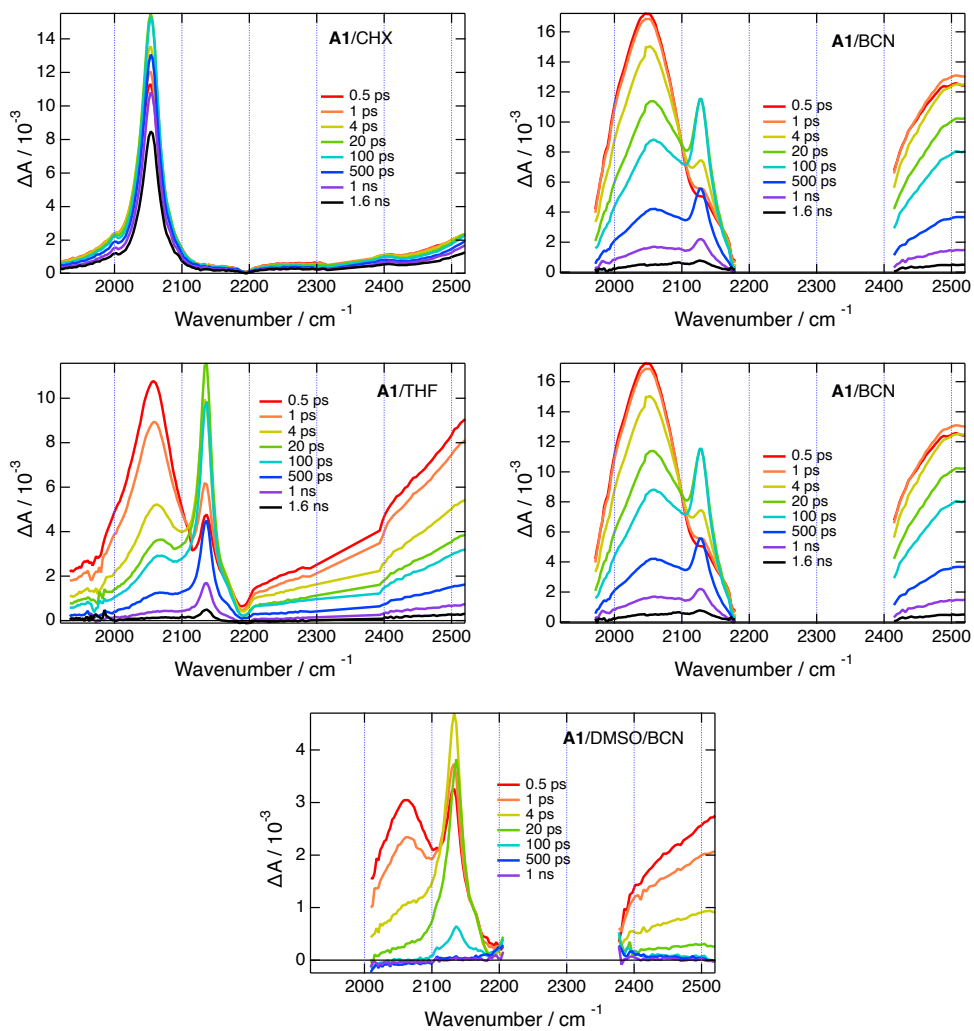


Figure S12 Time-resolved IR absorption spectra measured at various time delays after 600 nm excitation of **A1** in cyclohexane, toluene, tetrahydrofuran, benzonitrile and a 80:20 (v/v) dimethylsulfoxide/benzonitrile mixture.

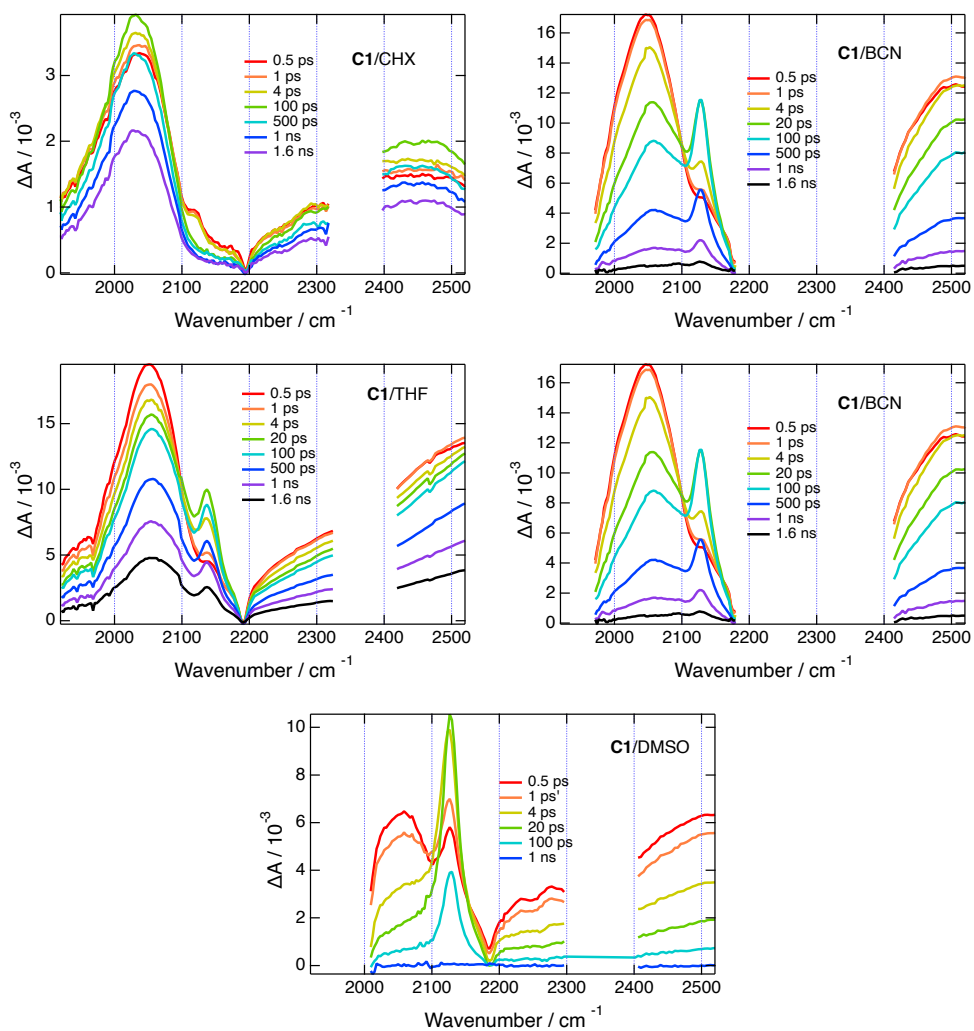


Figure S13 Time-resolved IR absorption spectra measured at various time delays after 640 nm excitation of **C1** in cyclohexane, toluene, tetrahydrofuran, benzonitrile and dimethylsulfoxide.

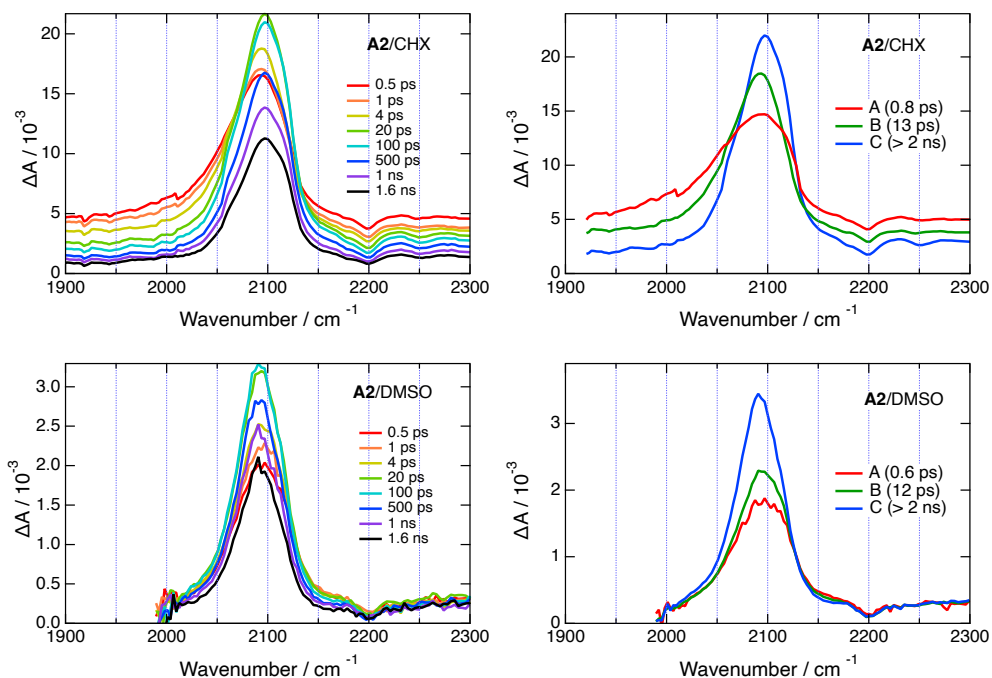


Figure S14 Left: time-resolved IR absorption spectra measured at various time delays after 565 nm excitation of **A2** in cyclohexane and dimethylsulfoxide. Right: Evolution-associated difference absorption spectra and time constants obtained from global analysis assuming a series of successive exponential steps (A→B→C→).

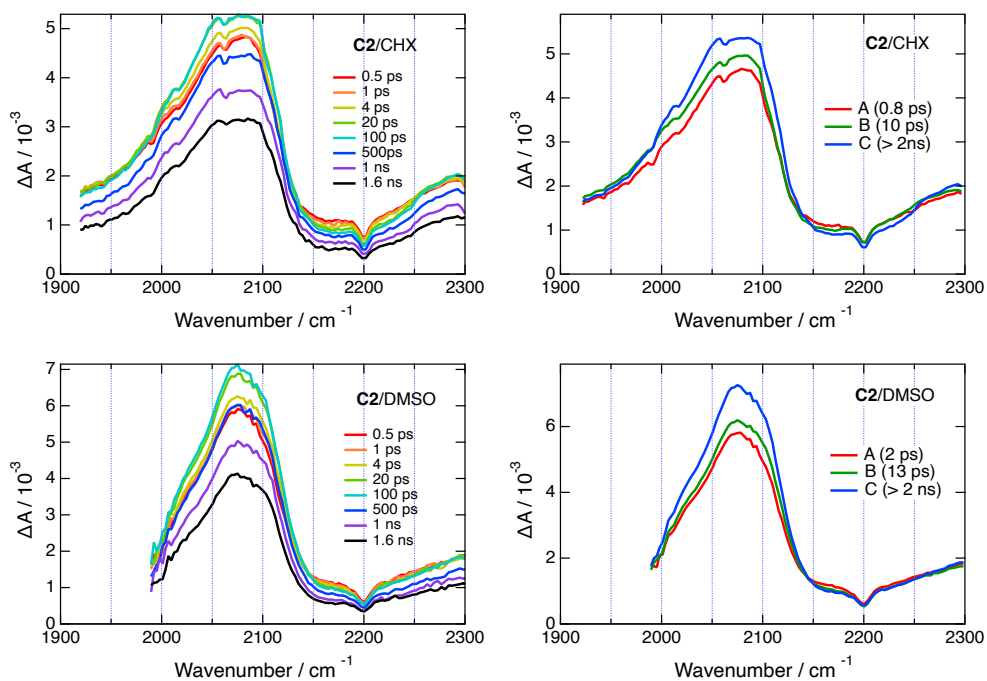


Figure S15 Left: time-resolved IR absorption spectra measured at various time delays after 600 nm excitation of **C2** in cyclohexane and dimethylsulfoxide. Right: Evolution-associated difference absorption spectra and time constants obtained from global analysis assuming a series of successive exponential steps (A→B→C→).

References

- [1] M. Grzybowski, I. Deperasińska, M. Chotkowski, M. Banasiewicz, A. Makarewicz, B. Kozankiewicz and D. T. Gryko, *Chem. Commun.*, 2016, **52**, 5108–5111.
- [2] K. Skonieczny, L. Kielesinski, M. Grzybowski and D. T. Gryko, *Chem. Commun.*, 2025, **61**, 5602–5606.
- [3] D. Rehm and A. Weller, *Isr. J. Chem.*, 1970, **8**, 259–271.